

Validation of DNS techniques for dynamic combined indoor air and constructions simulations using an experimental scale model

T.A.J. (Dennis) van Goch & A. W. M. (Jos) van Schijndel (corresponding author)

Eindhoven University of Technology

P.O. Box 513; 5600 MB Eindhoven; Netherlands, A.W.M.v.Schijndel@tue.nl

Abstract: This paper presents a study on the application of Direct Numerical Solving (DNS) techniques using an experimental scale model. The COMSOL Multiphysics software is promising in solving dynamic heat and air transport. However, the authors were not able to reproduce in 3D the experimental results using DNS, default grids and 32 GB of memory. This could mean that the current experimental scale model, with dimensions 0.64m x 0.45m x 0.39m, is practically already too big. This is also indicated by the fact that more reliable simulation results were obtained if each length scale was reduced with a factor 10 smaller than the current situation. Nevertheless, the experiments can be very useful as benchmark for CFD codes.

Keywords: DNS, scale, model, validation, indoor air

1. Introduction

The main purpose of the research is to develop a computational model for multi dimensional transient Heat, Air and Moisture (HAM) transport in buildings. This overall project intends to produce a tool that enables building performance based design. This paper is restricted to the modeling of the airflow in a (small scale) room as well as the temperature distribution in its construction (i.e. the moisture transport is left over for future research). After a literature study it was concluded that: (1) For full size buildings, turbulence models are necessary to solve CFD equations. One of the problems is that there are a lot of different turbulence models and they all give more or less different results. (2) Without turbulence modeling (i.e. Direct Numerical Solving (DNS) techniques), accurate results on turbulent flow can only be obtained using very small domains compared to buildings. (3) For DNS the following statement seems to be valid: The smaller the turbulence the bigger the domain that can be handled. (4) Another problem is the grid dependency of the solution. This

gives rise to the following main research question: "At what scale is the DNS technique still usable in relation with indoor airflow?" The research approach was as follows: The first step was to estimate the scale of the experiment for which DNS would still be usable. The second step was the design and building of scale model with (1) a substantial temperature difference (20 °C) between inside and outside; (2) a controllable and uniform heating device; (3) transparent construction for visualization of the airflow; (4) the presence of a cold surface; (5) temperature sensors; (6) infrared thermal imaging.

This paper presents is constructed as follows: Section 2 provides the design of the scale model and the measurements. Section 3 shows the 2D and 3D modeling results using COMSOL including a comparison with the measurements. The discussion is presented in Section 4.

2. The experimental scale model

2.1 Design

Figure 1 shows the experimental scale model, with external dimensions 0.64m x 0.45m x 0.39m. Each length scale (i.e. x, y, z) is a factor 7.7 smaller than the well documented full scale room experiment of Lu et al. (1997).

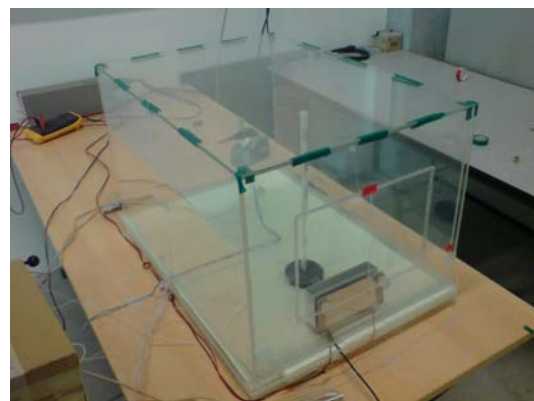


Figure 1. The experimental scale model

The dimensions are shown in figure 2.

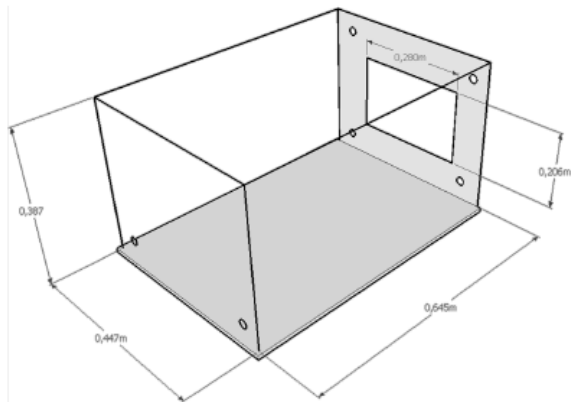


Figure 2. The dimensions of the scale model.

The sides and top of the box are constructed as follows: 3 mm plexiglass – 4 mm air cavity – 3 mm plexiglass. The material properties of plexiglass are: heat conductivity equals 0.21 W/mK, density is 1190 kg/m³, heat capacity equals 1500 J/kgK. The window and bottom are made of 4 and 6 mm plexiglass respectively.

The heating source is designed using an aluminum heat exchanger, as shown in figure 3.

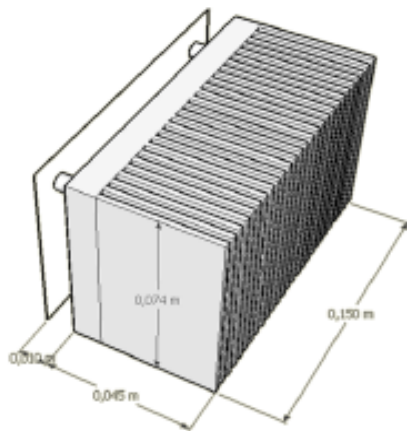


Figure 3. The aluminum heat exchanger.

Five electrical resistances of 1.1 Ohm each are mounted at the back of the aluminum block. Details on the positioning can be found in (van Goch 2008)

In order to control the inside temperature, a sensor (thermostat) is placed in the centre, 2 mm from the wall facing the window. Two more sensors are used to measure the surface temperature of the heat source and surroundings.

A data acquisition system is used for analog input of the just mentioned sensors and output for controlling the electrical power source connected to the electrical resistances. An on/off application has been implemented in Labview. Figure 4 shows an impression of this application.

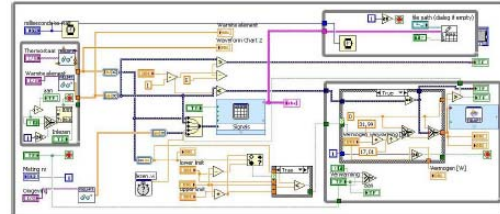


Figure 4. The on/off application in Labview.

After completion, the scale model and controller were tested on its functionality. Figure 5 shows a typical result. The curve at the top shows that the temperature of the heating source is switching between roughly 70 and 80 °C. The thermostat was set to 27 °C.

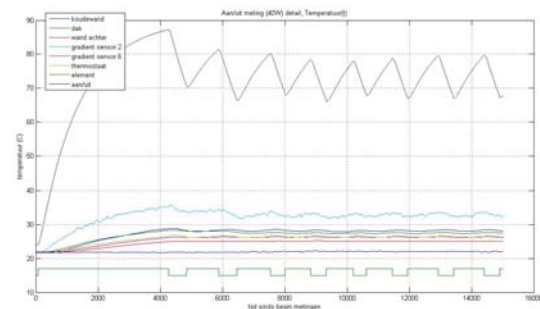


Figure 5. A test of the scale model and controller

2.2 Measurements

Three different types of measurements, thermal imaging, air flow visualization using smoke, time series of temperature sensors, were done.

2.2.1 Thermal imaging

Thermal images were obtained of the external side including the windows (front). These images are very useful for validation purposes because they show a 2D distribution over time. Figure 6 shows 4 images A through D using a heat source of 30 W. The controller was set on at all times, providing a step change over time. The time steps are: A 10 min; B 30 min; C 60 min; D 120 min.

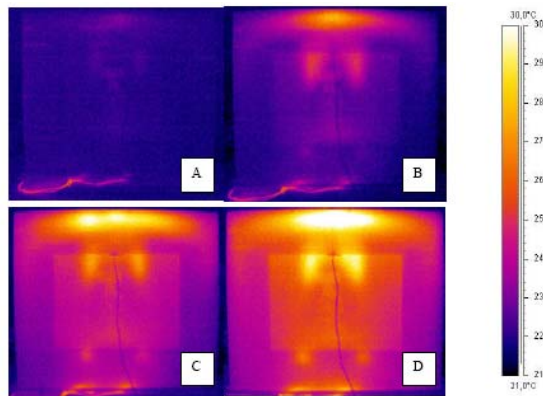


Figure 6. Thermal images of the external front

2.2.2 Flow visualization

The previous mentioned thermal images provide some indication of the air flow patterns inside the box. In order to get more detailed information on the inside air flow, smoke is injected using a small entrance near the bottom of the heating source. Figure 7 shows a typical result during steady state (after 120 min and 30W input power)

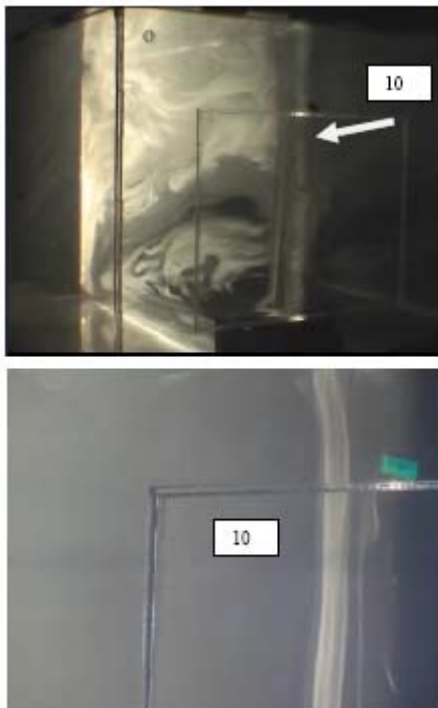


Figure 7. Air movement straight upwards Top: panoramic overview; bottom; front overview

In figure 8 the observed flow in the centre of the box is schematically shown:

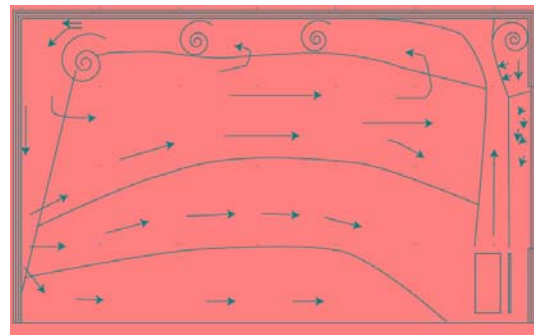


Figure 8. A schematic impression of the air flow at 'straight upward' configuration'

It is observed that the air flow reaches a stable state. The flow of figure 8 ('straight upward') is not representative on a wide range. A quite different pattern (see figure 9, ('attracted to window')) is observed 3 cm out of the centre.

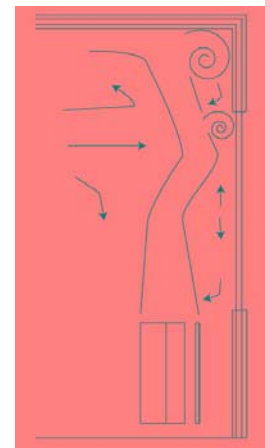


Figure 9. Airflow pattern 'attracted to window'

Due to this 3D effect, it is expected that 2D models will be not be able to simulate the flow accurately.

2.2.3 Time series

Temperature sensors (NTC) are placed at all centers of all sides of the box. At the inside, the temperature gradients are measured, using one hollow plexiglass pillar as shown in figure 10. The pillar is placed on several locations as provided in figure 11.

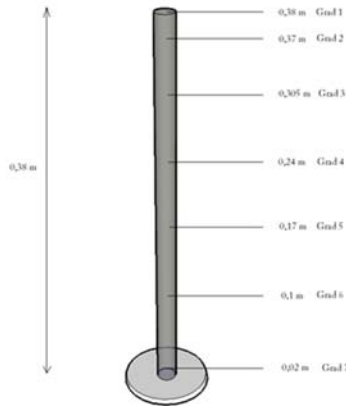


Figure 10. The locations of sensors at the pillar

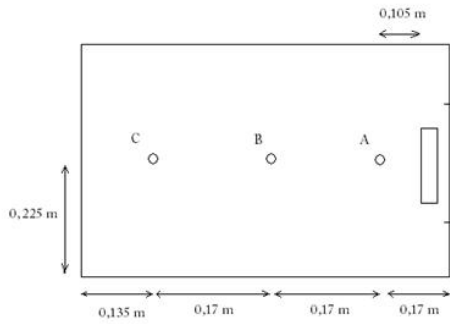


Figure 11. The locations of the pillar inside the box

A typical result of the outcome of these type of measurements has already been shown in figure 5.

3. Use of COMSOL Multiphysics

The combination of the ‘Convection and Conduction’ and ‘Navier-Stokes’ application modes are used to model and simulate the experiments. Due to our research question, the $k-\epsilon$ turbulence model is not used. Furthermore only default grids (course, fine, etc.) and solvers are used. The calculations were limited to a maximum of 32 GB memory at a Sun computer. At this point we want to emphasize that so far we are not able to simulate the experimental scale model, fully 1:1 in 2D/3D using COMSOL yet. Therefore we present the results of models that were more or less successful. In 2D we show the results of 1:4 model scales. In 3D we present the results of a 1:4 scale. Details of the model will be shown in the following Section. The other

models are similar and thus only simulation results will be provided.

3.1 2D Scale 1:4 results

Figure 12 presents the geometry and domains.

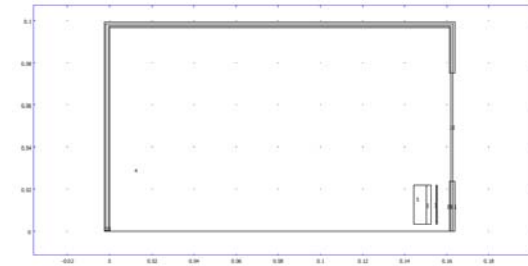


Figure 12. Geometry and domains

Figure 13 provides the boundary conditions

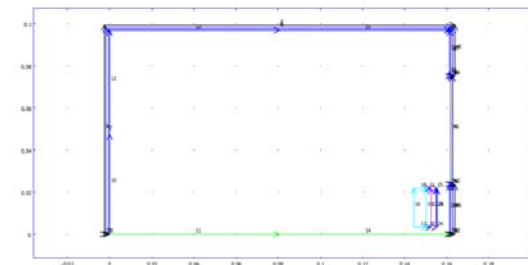


Figure 13. Boundary conditions

Figure 14 shows the mesh (refinement: Normal)

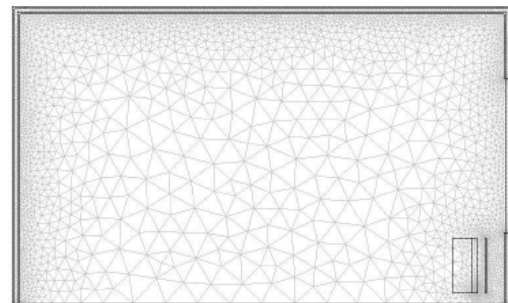


Figure 14. The mesh

The domain and boundary properties are presented in the following tables.

Table I. Sub domain settings

Subdomain		1, 3, 8, 10-11	2, 9	4		
Thermal conductivity (k)	W/(m·K)	0.21	0.024	0.024		
Density (rho)	kg/m ³	1190	1.293	1.293		
Heat capacity at constant pressure (C)	J/(kg·K)	1500	1007	1007		
x-velocity (u)	m/s	0	0	u		
y-velocity (v)	m/s	0	0	v		
Subdomain			5	6-7		
Thermal conductivity (k)	W/(m·K)		257	257		
Density (rho)	kg/m ³		1350	2700		
Heat capacity at constant pressure (C)	J/(kg·K)		880	880		
x-velocity (u)	m/s		0	0		
y-velocity (v)	m/s		0	0		
Subdomain initial value		1, 3, 8, 10-11	2, 9	4	5	6-7
Temperature (T)	K	295.15	295.15	295.15	295.15	295.15
Subdomain				4		
Integration order (gporder)				4	4	2
Constraint order (cporder)				2	2	1
Density (rho)	kg/m ³			rho_cc		
Dynamic viscosity (eta)	Pa·s			0.000015		
Volume force, y-dir. (F_y)	N/m ³			rho_cc*g*(T-Tl)*alpha1		
Subdomain initial value				4		
Pressure (p)	Pa			101000		

Table II. Boundary settings

Boundary		1-3, 5, 8, 28, 34, 40-42, 44-46	4, 6-7, 9-10, 12-13, 15, 20-21, 23-27, 29-33, 35-39, 43	11, 14
Type		Heat flux	Continuity	Thermal insulation
Inward heat flux (q0)	W/m ²	-h1*(T-Tl)	0	-h1*(T-Tl)
Temperature (T0)	K	0	0	0
Boundary			16-19	22
Type			Continuity	Temperature
Inward heat flux (q0)	W/m ²		0	0
Temperature (T0)	K		Twand_t	Twand_t
Boundary		10-18, 20-27, 29-32, 35		
Type		Wall		

Table III. Constants and expressions

Name	Description	Expression
rho1	Air density	1.293
Cp1	Air heat capacity	1007
lapl	Heat cond. plexiglass	0.21
lalu	Heat cond. air	0.024
Th	Initial temperature	293.15
rho2	Plexiglass density	1190
Cp2	Plexiglass heat cap.	1200
epsilon	Emissivity	0.9
Tamb	Ambient temperature	273.15
g	Gravitational acc.	9.81
eta	Air kin. viscosity	1.7e-5
alpha1	Air Lin. Exp. Coef.	3.2e-3
Rs	Gas Constant	286.9
h1	Heat transfer Coef.	8
Twand_t		-55.8*((2.71828183)^(t/1250))+350.95

Table III. Mesh statistics and solver options

Number of degrees of freedom	41353
Number of mesh points	4372
Number of elements	8353
Triangular	8353
Quadrilateral	0
Number of boundary elements	1439
Number of vertex elements	39
Minimum element quality	0.619
Element area ratio	0
Analysis type	Transient
Auto select solver	On
Solver	Time dependent
Solution form	Automatic
Symmetric	auto
Adaption	Off
Pivot threshold	0.1
Preordering algorithm	Minimum degree
Times	0:20:7200
Relative tolerance	0.01
Absolute tolerance	0.0010
Times to store in output	Specified times
Time steps taken by solver	Free
Manual tuning of step size	Off
Initial time step	1E-6
Maximum time step	1.0
Maximum BDF order	5
Singular mass matrix	Maybe
Consistent initialization of DAE systems	Backward Euler
Error estimation strategy	Exclude algebraic
Allow complex numbers	Off

Figure 15 shows the temperature distributions at four time steps

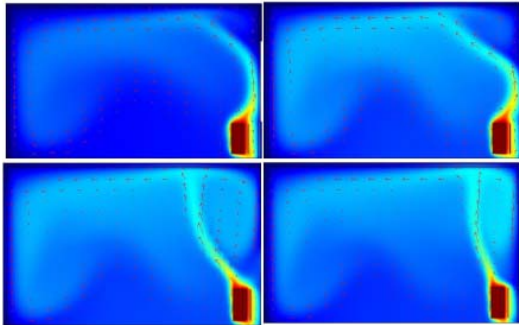


Figure 15. The air temperature after 15 min (upper left), 30 min (upper right), 1 hour (lower left) and 2 hours (lower right)

Figure 16 provides the air velocity distribution.

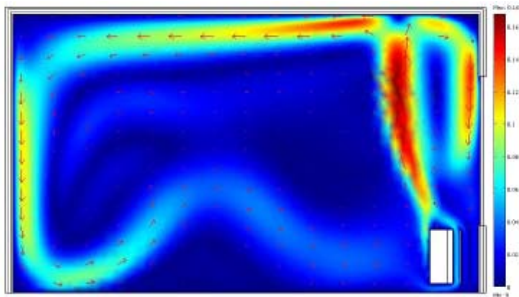


Figure 16. The air velocity distribution after 1 hour.

Figures 15 and 16 show that the solution is close to the measured ‘straight upward’ flow of figure 8. Furthermore, refining the grid ones, gives another solution more close to figure 9 with the airflow pattern ‘attracted to window’. This shown in figure 17.

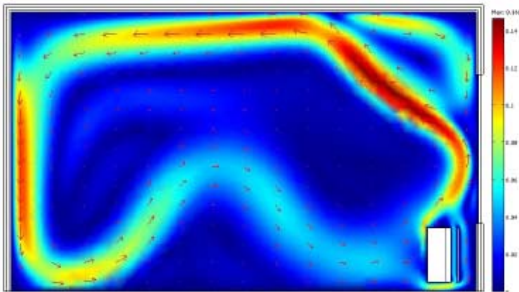


Figure 17. The air velocity distribution after 1 hour with a refined grid.

3.2 2D Scale 1:4 versus measurements

The temperature inside at the centre of windows and top side are selected for comparison. Figure 18 and 19 show the results.

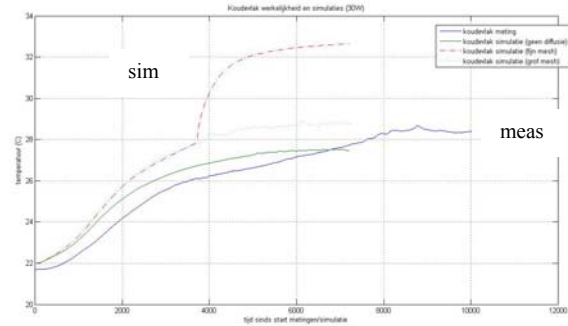


Figure 18. Simulated (with 3 different grids) and measured window temperature

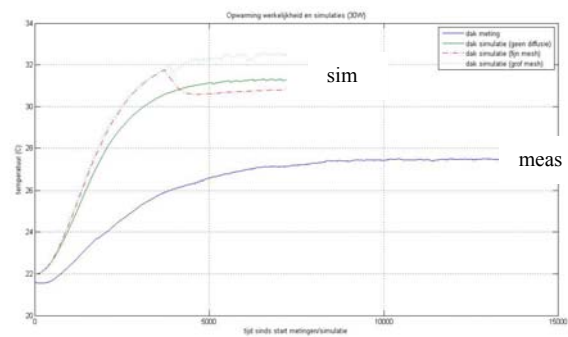


Figure 19. Simulated (with 3 different grids) and measured top side temperature.

Especially from figure 9 it is shown that the simulation results are not in agreement with the measurements. Furthermore, the simulated air velocities are about a factor 5 lower than the measured ones.

Although 2D, we expected the simulation results to be more close to the measurements. After evaluation of all results we have come to the conclusion that probably the modeling of the heating source is the main reason for the discrepancy between simulation and model. The simulated air velocity is simply too low just above the heating coil. Probably it is better to model the heating source using a velocity profile instead of natural convection.

3.3 3D Scale 1:4 results

In figure 20 the 3D geometry is shown.

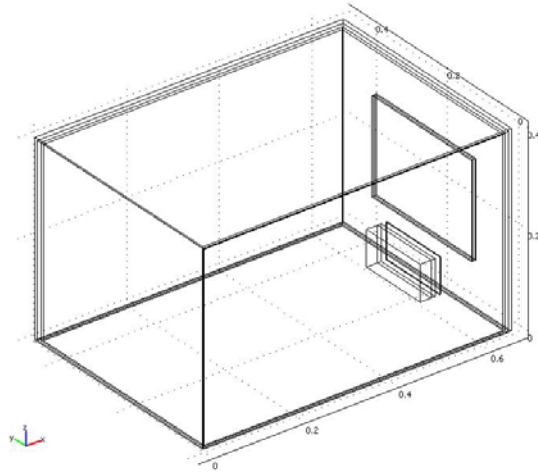


Figure 20. The 3D (1:1) geometry

With the 3D results it is possible to compare thermal images with simulations. The measured and simulated surface temperatures are provided in figure 21 (steady state) and 22 (after 900 seconds 'as good as it gets')

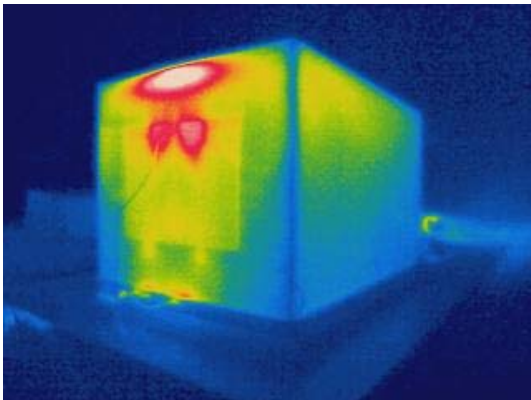


Figure 21. Measured surface temperature

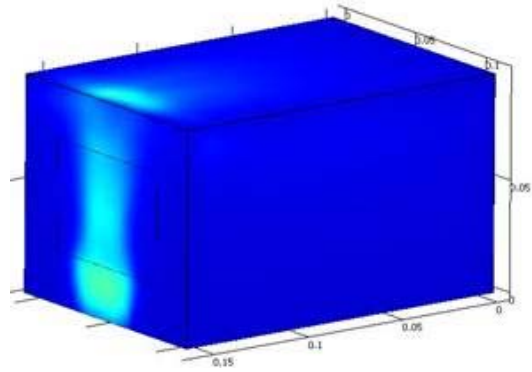


Figure 22. Simulated surface temperature

Figure 23 shows the temperature and velocity after 900 seconds.

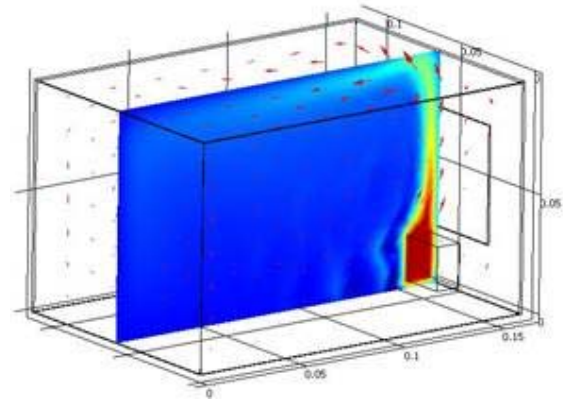


Figure 23. The temperature and velocity after 900 seconds.

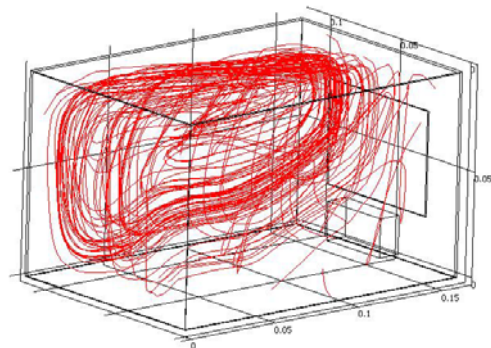


Figure 24. The air circulation

After this point the 3D simulation becomes unstable. However, 2D simulations (with its limitations of course) are capable to cover the whole time range.

4. Discussion

After evaluation of all results we have come to the conclusion that probably the modeling of the heating source is the main reason for the discrepancy between simulation and model. The simulated air velocity is simply too low just above the heating coil. Probably it is better to model the heating source using a velocity profile instead of natural convection.

Nevertheless, the COMSOL Multiphysics software is promising in solving dynamic heat and air transport. However, the authors were not able to reproduce in 3D the experimental results using DNS, default grids and 32 GB of memory. This could mean that the current experimental scale model, with dimensions 0.64m x 0.45m x 0.39m, is practically already too big. This is also indicated by the fact that more reliable simulation results were obtained if each length scale was reduced with a factor 10 smaller than the current situation.

6. Future Research

Future plans are to publish the current results as a benchmark and to improve the Comsol simulation results. If the latter is not successful, an even smaller experimental scale model is considered.

References

- Goch, T.A.J. van, (2008) Simulation and validation of heat and airflow in an experimental scale model. BSc thesis (In Dutch), University of Technology; fac. Building and architecture, BPS, 106 pages
HAMLab (2008) , <http://sts.bwk.tue.nl/hamlab/>
Lu, W., Howarth, A.T., Jeary, A.P. (1997). Prediction of airflow and temperature field in a room with convective heat source, Building and Environment 32(6) pp541-550
Schijndel A.W.M. van (2006), Heat, Air and Moisture Construction modeling using COMSOL with MatLab, Modeling guide version 1.0, Proceedings of the COMSOL Users Conference 2006 Eindhoven
Schijndel A.W.M. van (2007), Integrated Heat Air and Moisture Modeling and Simulation, Bouwstenen 116, ISBN: 90-6814-604-1, Eindhoven University of Technology